

# The Dynamics of Quantum Fluids

Henri Godfrin and Eckhard Krotschek

June 14, 2022

## Abstract

We review experimental and theoretical progress in the physical description of the dynamics of the quantum fluids  $^4\text{He}$  and  $^3\text{He}$ . Historically, the elementary excitations in these systems have been identified as phonons and rotons and, in  $^3\text{He}$ , collective zero sound and spin-fluctuations. Both recent high-precision measurements and theoretical methods have shown that the dynamics of these systems is actually very rich as will be discussed in detail in the body of this contribution.

**Keywords**— Quantum Fluids, Liquid Helium, Fermions, Bosons, Neutron Scattering, X-Ray scattering, Elementary Excitations, Phonons, Roton, Ripplons

## 1 The Helium Liquids

Helium ( $^4\text{He}$  and the less common isotope  $^3\text{He}$ ) and hydrogen are simple condensed matter systems, amenable to fundamental quantum mechanical descriptions. Helium remains liquid even at the absolute zero of temperature, an effect explained by Heisenberg's uncertainty principle, which has the consequence that light atoms confined in a small volume have a large kinetic energy, as is the case in a liquid or a solid, where each atom is confined by several surrounding atoms. For this reason, in helium, kinetic energies are larger than the weak interatomic potential energy. Even at the lowest temperatures, substantial atomic motion is present, and the system remains liquid, unless pressures on the order of 25 MPa are applied, and solidification is achieved. Another quantum effect plays an important role in the behavior of liquid helium: as the temperature is reduced below a few degrees Kelvin, the thermal de Broglie

wave-length of the atoms becomes larger than the interatomic distance. The waves describing the helium atoms overlap significantly, and a description in terms of individual wave-packets of distinguishable particles becomes inappropriate, it must be replaced by a quantum many-body description in terms of indistinguishable particles, governed by quantum statistics.

Quantum Mechanics and Statistical Physics [1, 2] explain well the properties of Quantum Gases, *i.e.* ensembles of non-interacting particles, which necessarily belong to one of the two possible classes: Bosons having an integer spin quantum number  $s$ ), or fermions with half-integer spin.  $^4\text{He}$  atoms ( $s=0$ ) are bosons, and  $^3\text{He}$  atoms ( $s=\frac{1}{2}$ ) are fermions.

The wave-functions of particles confined in a volume  $V$  are quantized plane waves characterized by their wave-vector  $\mathbf{k}$ . As shown by A. Einstein, the ground state of a Bose gas is the BEC (Bose-

Einstein condensate), where all particles occupy the same microscopic state with  $\mathbf{k}=0$ . The ground state of a Fermi gas is very different, because Pauli's principle forbids double occupancy for Fermions: the particles form a Fermi sphere in wave-vector space, by completing successive energy levels of increasing wave-vector, up to the Fermi wave-vector  $k_F$ . The energy  $E_F$  of the last one, called the Fermi level, can be considerable.

The excitation spectrum  $\epsilon(k)$  of these quantum gases is simply given by the kinetic energies of the individual particles,  $\epsilon(k) = \hbar^2 k^2 / 2m$ , where  $m$  is the particle mass and  $k$  the wave number. For bosons, at low temperatures, particles are excited from the common ground state. The energy spectrum is the usual parabolic spectrum of free particles described above. This behavior, however, is profoundly modified by interparticle interactions, *i.e.*, as is the case in Quantum Fluids [1, 2, 3, 4].

The Helium quantum *fluids* are unique in the sense that they are *very dense* and *very quantum*, making them a very challenging problem for theory. The issue is made quantitative by looking at the simple Lennard-Jones model of the helium fluids. In this model, the helium atoms interact via the interaction

$$V(r) = 4\epsilon \left[ \left( \frac{\sigma}{r} \right)^{12} - \left( \frac{\sigma}{r} \right)^6 \right] \equiv \epsilon v \left( \frac{r}{\sigma} \right)$$

where  $\epsilon = 10.22$  K is the well depth of the potential and  $\sigma = 2.556$  Å is the core size [5].

The interaction is not the very best (quantitative calculations are in fact made using the Aziz potential [6]), but it reproduces the ground state properties of the liquids within a few percent. Measuring all energies in units of the well depth, and all lengths in units of the core size,

$x \equiv r/\sigma$ , the Hamiltonian of the system is

$$\frac{1}{\epsilon} H(\mathbf{x}_1 \dots, \mathbf{x}_N) = \quad (1)$$

$$- \frac{\Lambda^2}{8\pi^2} \sum_i \nabla_{\mathbf{x}_i}^2 + \sum_{i < j} v(|\mathbf{x}_i - \mathbf{x}_j|)$$

where

$$\Lambda = \left( \frac{h}{m\epsilon\sigma^2} \right)^{\frac{1}{2}}$$

is de Boer's "quantum parameter" [7]  $\Lambda$ , giving the ratio between the de Broglie wavelength and a typical diameter of the molecule.  $\Lambda \approx 2.67$  for  $^4\text{He}$ ,  $\Lambda \approx 3.09$  for  $^3\text{He}$ , but  $\Lambda \approx 1.3 - 1.7$  for  $\text{H}_2$ ,  $\text{HD}$ ,  $\text{D}_2$ , and  $\Lambda < 0.1$  for heavy rare gases.

Moreover, the density of  $^4\text{He}$  at zero pressure is  $\rho_0 = 0.02185 \text{ Å}^{-3} = 0.365/\sigma^{-3}$  and for  $^3\text{He}$   $\rho_0 = 0.0163 \text{ Å}^{-3} = 0.273/\sigma^{-3}$ , in other words the average particle distance is of the order of the core size.

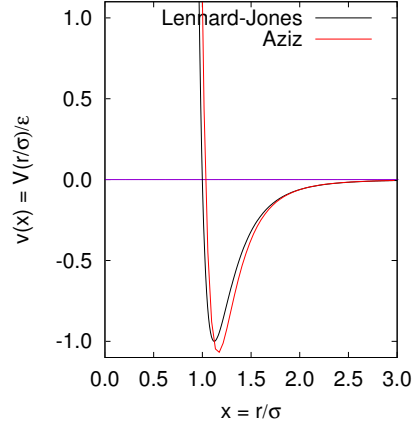


Figure 1: Normalized Lennard-Jones "6-12" interatomic potential, as a function of the normalized interatomic distance. The normalization factors for distances ( $\sigma$ ) and potential energies ( $\epsilon$ ) are given in the text. We also show, for comparison, the Aziz potential [6] which is the currently accepted most accurate static 2-body interaction.

## 2 $^4\text{He}$ in 3D

Liquid helium ( $^4\text{He}$ ) is the archetype of a Bose Liquid. Immediately after the discovery of the superfluidity of helium [8, 9] by Kapitza (Moscow) and Allen and Misener (Toronto), F. London [10] understood that the system was undergoing Bose-Einstein condensation, and L. Tisza proposed a “two-fluids model” featuring a coexistence of a normal fluid and a superfluid [4]. A Bose-Einstein condensed gas is not superfluid, however, and therefore the superfluidity observed in helium is an additional effect, associated to the interactions. A major step in the understanding of the physics of helium was made by L.D. Landau, who found a deeper interpretation of Tisza’s two-fluids model. Landau postulated that the “normal fraction”, which carries the entropy, is in fact the ensemble of thermal excitations of the superfluid ground state. This interpretation removed the unphysical consideration of two categories within a set of indistinguishable atoms. Landau considered elementary excitations of the fluid, in the form of quantized density fluctuations (“phonons”), similar to the Debye phonon modes of a crystalline solid. In order to calculate the thermodynamic properties by a Debye-like approach, where the energy is obtained by a sum over all modes, weighted by the Bose factor, Landau postulated that the dispersion relation  $\epsilon(k)$  had a linear part  $\epsilon = \hbar ck$ , where  $c$  is the speed of sound, and another part displaying a minimum, the “roton gap” of energy  $\Delta$ . Landau’s intuition was guided by specific heat measurements, showing a cubic temperature dependence at low temperatures (below 0.5 K), as expected from the linear part of the dispersion relation, as well as an exponential contribution at higher temperatures (on the order of 1K), characteristic of an energy gap.

In a first article [11], Landau proposed a spectrum with two branches, with a parabolic branch centered at  $k=0$  in addition to the linear branch. This spec-

trum was not found satisfactory by Landau himself, the presence of two branches being reminiscent of Tisza’s “two kinds of atoms”.

In a second publication [12], he presented his celebrated “Landau dispersion relation”, where a single branch of excitations characterizes the full spectrum (Fig. 2). With two parameters, the sound velocity  $c$  and the roton gap  $\Delta$ , both obtained from the temperature dependence of the specific heat, Landau’s theory provides an excellent account of the experimental properties of superfluid helium at low temperatures. The existence of a “second sound” collective mode, where the superfluid and normal components oscillate with opposite phases while keeping the total density constant, as proposed by Tisza, corresponds in Landau’s model to propagating entropy (and hence temperature) waves.

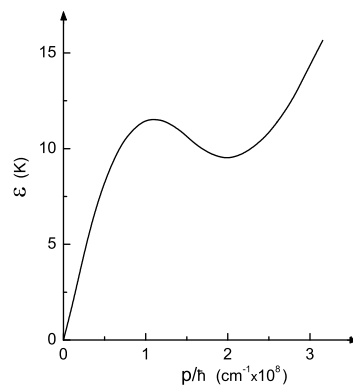


Figure 2: The dispersion relation proposed by L. D. Landau in 1947 to describe the elementary excitations in superfluid  $^4\text{He}$  at zero pressure.

Another fundamental observation due to Landau, is that the particular shape of the dispersion relation leads to the superfluid behavior. A simple argument of energy and momentum conservation shows

that the creation of excitations by the displacement of an object immersed in the fluid is not possible, unless the object's velocity exceeds a critical value. The linearity of the dispersion relation at low wave vectors is essential for this to happen: in a Bose gas, where the dispersion relations is parabolic, the critical velocity is zero, the system remains normal even at the absolute zero of temperature. The evolution of the dispersion relation from the parabolic shape characteristic of a gas, to the linear behavior observed as the interaction is switched on, has been explained by Bogoliubov (1947) [13] in the weak interaction limit. The dispersion relation of the elementary excitations plays therefore a major role in the determination of the thermal properties, and also in the superfluid nature of the liquid's ground state.

Landau's phenomenological theory introduced the fruitful concept of "quasi-particles", describing in a simple way the elementary excitations of complex many-body systems. The concept was of course already present in the Debye theory of solids, but the generalization to helium, a non-periodic system of strongly interacting particles, opened a new field of physics.

There were however two serious interrogations after Landau's theory was released. The first was obviously related to the necessity of an experimental observation of the proposed dispersion curve. And the second, to the need of a microscopic theory providing some insight in the superfluid helium behavior, and able to test the validity of Landau's model.

Experimentally, the evidence for a Landau-like dispersion relation was missing: only indirect evidence obtained from thermodynamic measurement (specific heat, thermal conductivity, viscosity, fountain pressure, etc.) was available. Feynman and Cohen suggested the use of inelastic neutron scattering, a technique already used to measure phonon dispersion curves in crystals, to try to observe the excitation dispersion curve of super-

fluid helium. The first proof of the existence of a roton minimum was reported by H. Palevsky, K. Otnes, K. E. Larsson, R. Pauli and R. Stedman (1957) [16, 17], clearly showing that the elementary excitations in superfluid helium are extremely sharp, compared to those of normal helium. These exciting results motivated extensive investigations of the dynamics of helium, covering the low energy region, *i.e.* the Landau-like dispersion relation, the multi-excitations region at higher energies, as well as the very high energy region of the spectrum, where BEC can be investigated [18].

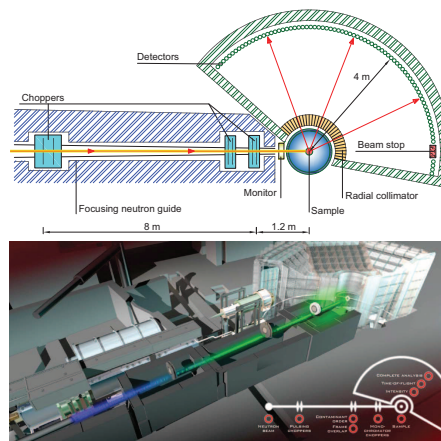


Figure 3: The time-of-flight neutron scattering spectrometer IN5 at the Institut Laue-Langevin.

The principle of the inelastic neutron scattering is simple, but measurements are demanding, and high flux neutron sources (reactors, spallation sources) are needed. The helium sample is placed in an incident beam of "monochromatic" (of a given energy) neutrons, which are scattered by the helium sample, and then detected at some distance from the sample, as a function of angle and time of arrival, in the so-called time-of-flight technique. Other methods (triple-axis, back-

scattering, spin-echo, etc.) have also been used, offering a different coverage of the momentum-energy plane, and also different resolutions in energy and momentum.

Energy and momentum conservation allow the determination of the energy transfer and the momentum transfer from the neutron to the helium sample, which correspond to the energy  $\epsilon = \hbar\omega$  and momentum  $\hbar\vec{k} = \hbar\vec{Q}$  of the density fluctuations created in the helium. The incident neutron has an energy  $E_i$  and a wave-vector  $\vec{k}_i$ , and, after scattering, a final energy  $E_f$  and a wave-vector  $\vec{k}_f$ ; the wave-vector transfer is  $\vec{Q} = \vec{k}_i - \vec{k}_f$ , and the energy transfer  $\hbar\omega = E_i - E_f$ . The first microscopic theory of superfluid helium, due to R. P. Feynman (1954) [14], is a wonderful example of physical intuition. He found a general form for a variational wave-function which successfully explained the general shape of the dispersion relation, including the roton minimum. It was soon completed by Feynman and Cohen [15], who introduced, improving the variational wave-functions, the concept of “backflow”: the flow of helium atoms around a moving helium atom.

Dealing with many-body correlations, including dynamic effects, has been central to the development of microscopic theories, which have been considerably refined in the last decades, reaching now a quantitative power of prediction, as shown below.

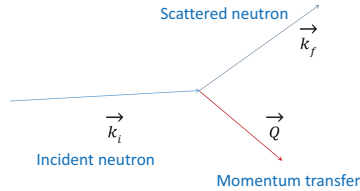


Figure 4: Neutron scattering: an incident neutron of wavevector  $\vec{k}_i$  creates an excitation of momentum  $\hbar\vec{k} = \hbar\vec{Q}$  in the superfluid.  $\vec{Q}$  is the wavevector transfer (see text)

The theory of neutron scattering [19, 20, 18] relates the double differential scattering cross section per target atom, which is the parameter measured by a scattering experiment, to the dynamic structure factor  $S(Q, \omega)$  and the dynamic susceptibility  $\chi(Q, \omega)$ , the latter being the functions calculated by microscopic theories. They are given by the following expression, where  $b_c$  is the coherent scattering length of helium:

$$\frac{\partial^2 \sigma}{\partial \Omega \partial E_f} = \frac{b_c^2}{\hbar} \frac{k_f}{k_i} S(Q, \omega) \quad (2)$$

Results are generally presented in terms of  $S(Q, \omega)$ , where sharp peaks of high intensity are observed, as expected from the creation of Landau “single-excitations”, as well as a more complex, broad landscape of multi-excitations. A vast literature on the subject exists, as described in the review articles by Woods and Cowley, Stirling, Glyde (see [18]), the book by Glyde [20], and recent works [21, 22], which benefited from the substantial progress of neutron scattering facilities and instruments.

The dispersion relation  $\epsilon(k)$  of the sharp single-excitations, as measured in recent inelastic neutron scattering experiments, is shown in Fig. 5. It closely resembles the curve predicted by Landau, with a linear part at low wave-vectors (“phonons”), and a deep gap (“roton” minimum) at a wave-vector  $k \sim 2.8 \text{ \AA}^{-1}$ . The name roton is historical, no special rotation takes place; the minimum in energy reflects an incipient localization (short-range order), which eventually will lead to a liquid-solid transition under a pressure  $P \sim 2.5 \text{ MPa}$ . The dispersion curve becomes flat for  $k \geq 2.8 \text{ \AA}^{-1}$  as the energy reaches twice the roton gap, forming “Pitaevskii’s plateau”.

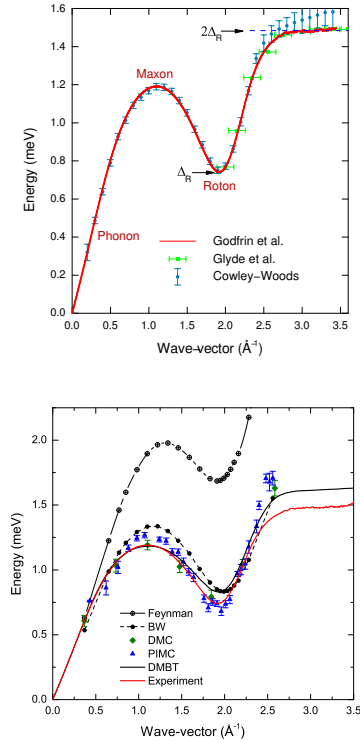


Figure 5: The dispersion relation  $\epsilon(k)$  of excitations in superfluid  $^4\text{He}$  at zero pressure. Top: Experimental data, displaying the phonon, roton, maxon, and plateau regions of the spectrum. The red dots are recent high-accuracy, highly pixelized data (seen at this scale as a continuous line, the dispersion is only visible at the highest wave-vectors) from Ref. [22], the blue dots with error bars are from the original work by Cowley and Woods [23] and the green dots from the high-momentum measurements by Glyde *et al.* [24]. Bottom: theoretical results, from Feynman’s model [14] to modern calculations such as Brillouin-Wigner perturbation theory with correlated wave function (BW, Ref. [25, 26]), diffusion (DMC [27, 28]) and path-integral (PIMC, [29]) Monte Carlo calculations and dynamic many-body theory (DMBT) [30, 21], compared to the experimental curve [22].

The calculation of the low temperature ( $T < 1.3\text{ K}$ ) thermodynamic properties of helium at low temperatures only involves the statistical physics of phonons and rotons of low energy. That is, the properties of the strongly interacting bosonic system are simply given by those of a collection of non-interacting bosonic “quasi-particles” described by the phonon-roton curve [22]. At high temperatures, where the number of rotons becomes very large, roton-roton interactions start playing a role. At the “lambda point” ( $T=2.17\text{ K}$ ),  $^4\text{He}$  becomes a normal fluid.

Theoretical studies of the dynamic structure function in  $^4\text{He}$  began with the work of Feynman [14] and Feynman and Cohen [15], the Feynman theory of elementary excitations was developed in a systematic Brillouin-Wigner perturbation theory by Jackson and Feenberg [31, 25, 32, 33] in terms of a basis of Feynman excitation states

$$\{|\mathbf{k}\rangle\} = \{S^{-1}(k)\hat{\rho}_{\mathbf{k}}|\Psi_0\rangle\} \quad (3)$$

where  $\hat{\rho}_{\mathbf{k}}$  is the density operator and  $|\Psi_0\rangle$  is the ground state. An important contribution was the identification of classes of theories for the dynamic structure function [34] that satisfy the  $\omega^0$  and  $\omega^1$  sum rules exactly. The most complete evaluation of the phonon-roton dispersion relation in terms of Brillouin-Wigner perturbation theory was carried out by Lee and Lee [26] who obtained an impressive agreement with the experimental phonon-roton spectrum up to the wave number of  $Q = 2.5\text{ \AA}^{-1}$ . The major drawback with these old calculations was that the required input – pair- and three-body distribution functions – were poorly known. Manousakis and Pandharipande [35] tried to generalize the input states of the Brillouin-Wigner perturbation theory to include “backflow” correlations in the spirit of Feynman and Cohen [15]. Through the gradient operator acting on the wave function, in principle dynamic correlations are introduced to all

orders. The “backflow-function” is, however, chosen per physical intuition rather than by fundamental principles, and the evaluation of the perturbative series becomes very complicated. Topologically, diagrams similar to those of Lee and Lee [26] were included. While the accuracy of the theoretical roton energy is comparable to that of Lee and Lee, one can clearly see an inconsistency since the energy of the Pitaevskii-plateau [36] lies be-

low twice the energy of the roton gap. More recent progress [37, 30] used a hybrid approach of Brillouin–Wigner perturbation theory and equations of motion for time-dependent multiparticle correlation functions to derive a self-consistent theory of the dynamic density-density response of  $^4\text{He}$ .

In a nutshell, the Feynman theory of excitations is generalized by writing the dynamic wave function as

$$\Psi(\mathbf{r}_1, \dots, \mathbf{r}_N; t) = \exp(U(t))\Psi_0(\mathbf{r}_1, \dots, \mathbf{r}_N) \quad (4a)$$

$$U(t) = \sum_i \delta u_1(\mathbf{r}_i; t) + \sum_{i < j} \delta u_2(\mathbf{r}_i, \mathbf{r}_j; t) + \dots \quad (4b)$$

The Feynman form of the wave function is obtained by omitting all  $n$ -body fluctuations  $\delta u_n(\mathbf{r}_1, \dots, \mathbf{r}_n; t)$  for  $n \geq 2$ . The different theoretical descriptions basically differ by the way the  $n$ -body fluctuations are determined.

Recent novel numerical methods [28, 27, 38, 39, 40] give access to dynamic properties of quantum fluids. These are important algorithmic developments that may ultimately aid in the demanding elimination of background and multiple-scattering events from the raw data. Of course, it is generally agreed upon that the model of static pair potentials like the Aziz interaction [6] describes the helium liquids accurately. Hence, given sufficiently elaborate algorithms and sufficient computing power, such calculations must reproduce the experimental data. The aim of the works cited above is different: The identification of physical effects like phonon-phonon, phonon-roton, roton-roton, maxon-roton ... couplings that lead to observable features in the dynamic structure function is, from simulation data, only possible a-posteriori whereas the semi-analytic methods permit a direct identification of these effects, their physical mechanisms, their relationship to the ground state structure, and

their consequences on the analytic properties of the dynamic structure function, directly from the theory.

The dynamic structure of  $^4\text{He}$  is actually quite rich as seen in Fig. 6 [30, 21]: “multi-excitations” are observed at energies above the single-excitation dispersion curve discussed above. They can be related to combinations of single-excitations, some of them are indicated in Fig. 6 by colored ellipses: in blue, an extension of the linear phonon region (“ghost phonon”) deep into the continuum; in red, an extension of the Pitaevskii-Plateau to small wave-vectors; in green, above the roton minimum, a broadening of the dispersion relation due to a Cherenkov effect; a red dashed ellipse at high energies indicates a region of maxon-roton couplings. Multi-excitations are well reproduced by recent theories. The mechanisms behind these are mostly the same: It is kinematically possible that a perturbation of energy/momentum  $(E, \mathbf{k})$  can decay into two sharp quasiparticle excitations. For example, the “ghost phonon” is caused by the effect that a perturbation can decay into two almost collinear phonons, hence the effect disappears at about twice the energy and wave number at which the dispersion

relation  $\epsilon(k)$  ceases to be linear. Similarly, the “Pitaevskii-Plateau” is caused by the effect that a perturbation of energy  $2\Delta$  can decay into two rotons of energy  $\Delta$  and wave number  $k_\Delta$ . Hence, energy and momentum conservation dictate that the plateau ends at a wave number of  $2k_\Delta$ , in this case the two roton wave vectors are parallel. Perturbations with the same energy and smaller wave numbers can decay into two rotons that are not

collinear. That means that the plateau can in principle extend to zero wave number; in that case the perturbation decays into two anti-parallel rotons.

The Cherenkov effect is particularly interesting; it is caused by the fact that the group velocity of a quasiparticle excitation beyond the roton ( $R_+$  roton) is larger than the sound velocity. The effect is observed only at low pressures.

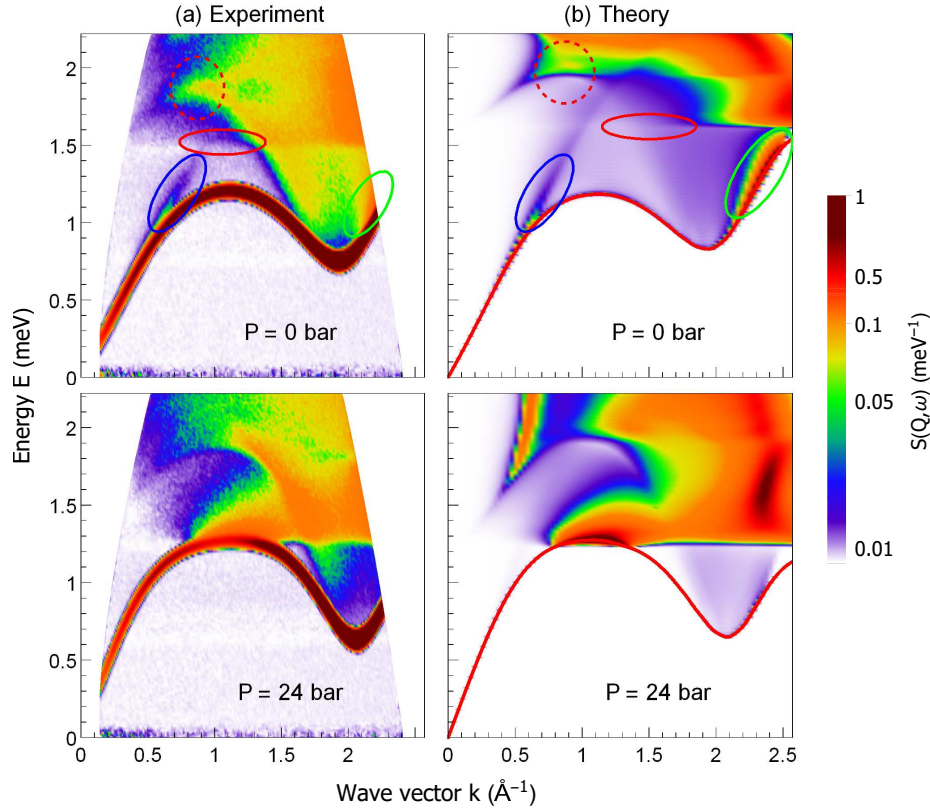


Figure 6: Experimental (left) and theoretical (right) determinations of the dynamic structure factor of superfluid  $^4\text{He}$  at zero pressure (upper graphs) and near-solidification pressure (lower graphs) [30, 21]. In addition to the the intense single-excitations dispersion seen in Fig. 5 (red lower curves), much lower intensity multi-excitations (see color scale) can be observed here. Colored ellipses indicate excitation couplings described in the text.



### 3 $^3\text{He}$ in 3D

The investigation of the dynamics of the  $^3\text{He}$  Fermi Liquid has naturally followed that of the  $^4\text{He}$  Bose fluid [41, 20]. From the theoretical point of view, the problem is notoriously difficult, due to the antisymmetry requirement for the wavefunctions of many-body fermionic systems [1, 2, 3]. Obtaining accurate results for the ground state is a challenge, even using very sophisticated variational wave functions.

The dynamics is treated analogously to the boson case (4b); the local excitation functions  $\delta u_n(\mathbf{r}_1, \dots, \mathbf{r}_n; t)$  are replaced by particle-hole operators

$$\sum_{\substack{p_1, \dots, p_n \\ h_1 \dots h_n}} u_{p_1, \dots, p_n; h_1 \dots h_n}(t) \times \\ \times a_{p_1}^\dagger \dots a_{p_n}^\dagger a_{h_n} \dots a_{h_1}$$

where the  $p_i$  are the quantum numbers of unoccupied (“particle”) states and the  $h_i$  those of occupied (“hole”) states. Restricting the excitation amplitudes to one-particle-one-hole components leads to a correlated version of the random phase approximation (RPA) [42], the quantitative understanding of the experiments requires at least 2-particle-2-hole amplitudes, see Refs. [43, 44].

From the experimental point of view, even though the same inelastic neutron techniques successfully applied to superfluid  $^4\text{He}$  can be used to investigate liquid  $^3\text{He}$ , in practice the experiments are extremely difficult due to the huge neutron absorption cross-section of the  $^3\text{He}$  nucleus [20]. In typical  $^4\text{He}$  experiments, sample thicknesses are larger than 1 cm, while absorption limits the maximum thickness in a liquid  $^3\text{He}$  measurement, to about 0.1 mm. In addition, due to the lower excitation energies, experiments in  $^3\text{He}$  must be performed at much lower temperatures ( $\approx 0.1$  K) than in  $^4\text{He}$  ( $\approx 1$  K), to remain in the low temperature limit, where few excitations are present.

For these reasons, in spite of the considerable interest in strongly interacting fermions, accurate theoretical and experimental results have been available only recently [45].

In order to understand the dynamics of a Fermi *liquid*, we begin by considering the excitations of a Fermi *gas*. In the latter, excitations are created by removing a particle from an occupied state inside the Fermi sphere, and placing it outside the sphere, in a higher energy free state. The resulting states are confined to a region of the energy *vs* wave-vector space called the “particle-hole band”. The interacting fermionic system, *i.e.* the Fermi Liquid, behaves in a similar way. A particle-hole band can be observed in bulk  $^3\text{He}$  (see Fig 7), but in addition, collective modes are present. A density mode, named “zero-sound” or “collision-less sound”, is observed. Its physical origin, as noted by D. Pines [46], resides in the strong interactions, and hence this mode is analogous to the phonon-roton mode described above for bosons; statistics play here a minor role. Its substantial energy width results from the possibility to decay into particle-hole excitations as it enters the particle-hole band (Landau-damping mechanism).

The thermodynamic properties of bulk liquid  $^3\text{He}$  are often described, at very low temperatures, by the phenomenological Landau Fermi Liquid model, where the properties of the interacting system are related to those of the Fermi gas by the introduction of an interaction function (“quasiparticle interaction”), leading to a renormalization of parameters (effective mass, susceptibility enhancement, etc.). Landau theory predicts, among other physical effects, the existence of collective modes, the zero-sound and paramagnon modes.

Landau’s Fermi Liquid Theory is only applicable at very low temperatures. In liquid  $^3\text{He}$ , where the Fermi energy, ex-

pressed in temperature units, is of the order of several kelvins, the theory is valid below 0.1 K.

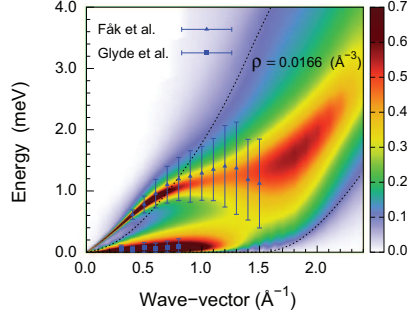


Figure 7: (Color online) Dynamic structure factor of bulk liquid  $^3\text{He}$ . Measured density excitations [47] (triangles, upper branch) and spin-density excitations [45] (squares, lower branch) are clearly visible (bars on the data points indicate the observed width of the branch). Color intensity map, from light blue to dark red: DMBT microscopic theory including exchange [44]. The solid lines indicate the boundaries of the particle-hole band.

The reason becomes clear if one observes the actual excitation spectrum shown in Fig. 7. The low energy mode, observed below the zero-sound excitation, is a spin-density mode, completely immersed in the particle-hole band, and hence severely Landau-damped. The origin of this mode, analogous to a dampened spin-wave and often called “paramagnon”, can be traced back directly to the antisymmetry of the many-body wave function.

There are also some interesting X-ray studies of the dynamic structure function at high momentum transfers [48] that have led to a discussion about the location of the particle-hole band [49, 50]. The authors of Ref. [48] state that *The obtained results show no evidence of such a decay: the zero-sound mode remains well defined in the whole explored wave number range.*

According to that, the particle-hole continuum should be much lower than the continuum of the non-interacting Fermi system. An analysis of both the data and the theoretical predictions within DMBT [51] shows that there is, when the theoretical data are convoluted with the experimental resolution, actually no contradiction to the conventional interpretation of the scenario.

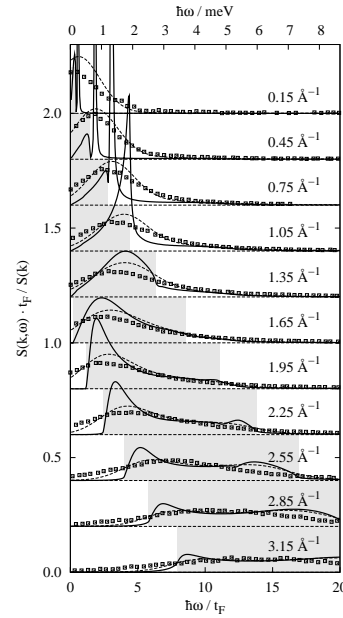


Figure 8: The figure shows the normalized dynamic structure function  $S(k, \omega)/S(k)$  of  $^3\text{He}$  at a density of  $\rho = 0.0166 \text{ \AA}^{-3}$ , for a sequence of wave numbers. The theoretical results obtained by DMBT [51] are compared with the X-ray scattering data [48] (squares) at saturated vapor pressure. Also shown are the theoretical results convoluted with the experimental resolution (dashed lines). The gray-shaded area shows the particle-hole continuum of a non-interacting Fermi fluid.  $t_F = \hbar^2 k_F^2 / 2m$  is the Fermi energy of the non-interacting system.

Details are shown in Fig. 8. To facilitate the comparison with experiments, the theoretical spectra were convoluted with the experimental resolution. Also, the results were scaled by  $1/S(k)$  such that the integrated strength is 1 for all momentum transfers. The same scaling was applied to the experimental data.

## 4 $^4\text{He}$ in reduced dimensions

The dynamics of quantum fluids has also been investigated in reduced dimensions. Two-dimensional (2D) systems are obtained experimentally by adsorp-

tion of gases onto solid substrates, usually graphite. One-dimensional (1D) systems can also be created, they are obtained by confining the gases inside silica or graphite nano-tubes [52, 53, 54]. There is also theoretical interest [55, 56, 57, 58, 59] in the properties of  $^4\text{He}$  in *one*-dimension.

Extensive theoretical studies have clarified the nature of the excitations in such systems. Superfluid  $^4\text{He}$  films of atomic thicknesses, for instance, display in-plane density modes, as well as capillary waves.

Let us first discuss the dynamics of rigorously 2D  $^4\text{He}$ . Basically we see the same effects as in 3D: a linear “phonon” branch as well as, at high momentum transfers, a “roton minimum”.

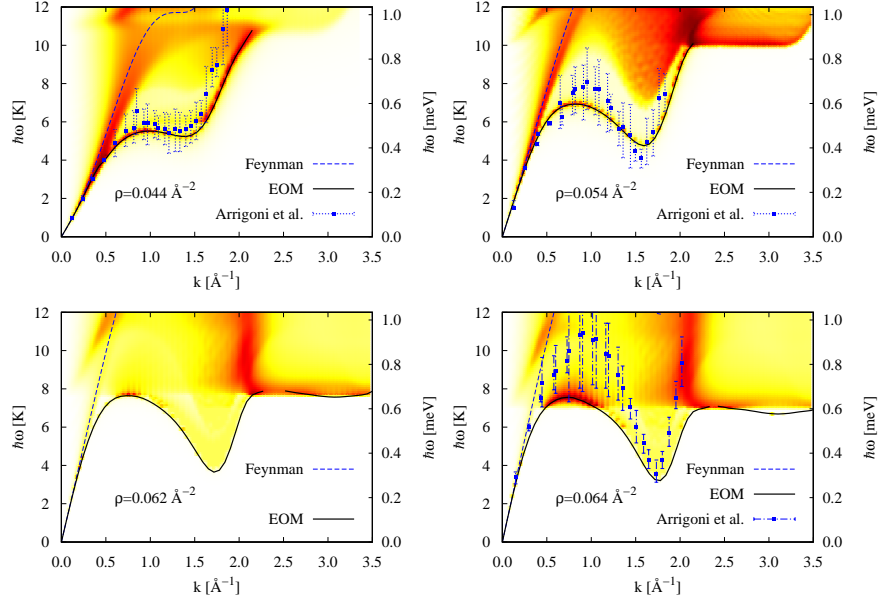


Figure 9: (Color online) The figure shows contour plots of the dynamic structure function of two-dimensional liquid  $^4\text{He}$  for a sequence of areal densities as shown in the legends. The colors have been chosen to highlight the prominent features, darker colors correspond to higher values of  $S(k, \hbar\omega)$ . We also show the Feynman spectrum, and the simulation data of Ref. [60]. From Ref. [61].

One can also see the somewhat finer details discussed above: At low densities, the “ghost-phonon”, and at high densities the plateau coming down and extending to long wave lengths. A second striking feature is the appearance of a sharp mode below the plateau. We stress the difference: normally, the plateau is a threshold above which a wave of energy/momentum ( $\hbar\omega, k$ ) can decay into two rotons. This has the consequence that the imaginary part of the self-energy  $\Sigma(k, \hbar\omega)$  is a step function and the real part has a logarithmic singularity [36]. A collective mode is, on the other hand, characterized by a singularity of the  $S(k, \hbar\omega)$ . Figs. 9 show, for the two highest densities, the appearance of a sharp discrete mode below the plateau. At a wave number of  $k \approx 2.6 \text{ \AA}^{-1}$ , the collective mode is still merged into the continuum. With increasing wave number, we see, however, a clearly distinguishable but rather weak ( $Z(k) \approx 0.02$ ) mode about 0.3 K below the plateau. We have mentioned already above that the roton should be seen as an emergence of short-ranged order, the “ghost of a Bragg Spot” [62, 63]. If this is the case, then one might see a second Bragg spot. Such a thing is not seen, but location of the secondary minimum in 2D corresponds indeed to the position of a second Bragg spot of a triangular lattice.

Density modes are analogous to the phonons and rotons already mentioned in the case of bulk helium, but due to the adsorption potential of the substrate, the fluid is inhomogeneous, and solidification of the first two or three atomic layers is observed in thick films. Layered-excitations are observed in this regime.

Capillary waves, also called “ripplons”, have a different nature: these are surface waves, which do not (in first approximation) correspond to compression/expansion of the fluid, but to a change of height in the external potential (gravitational in the case of a bulk helium surface, or substrate potential in adsorbed films).

A typical example is shown in Fig. 10. It corresponds to a multilayer film of about 6 atomic layers, where both density excitations and ripplons are visible with comparable intensity [64]. The experimental curve is broader than the theoretical one, an effect largely due to the mosaic spread (angular distribution) of the graphite substrate, a powder made of microscopic flat crystals.

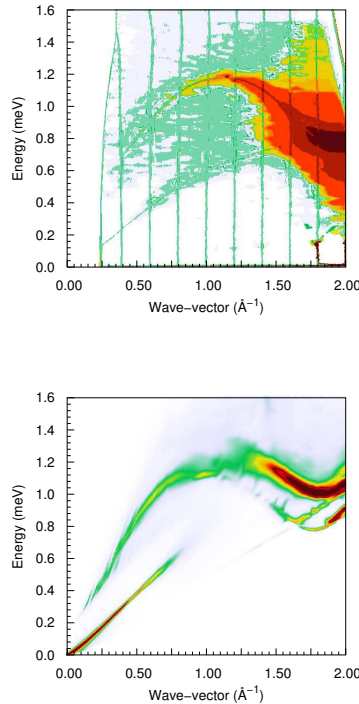


Figure 10: Experimental [64] (top) and theoretical (bottom) [65] determinations of the dynamic structure factor of a multilayer film of  $^4\text{He}$ , displaying density and ripplon excitations.

Finally, in the sub-monolayer coverage regime, one can observe gaseous, fluid and solid phases, as well as “commensurate phases” where the atoms adopt a periodic arrangement commensurate with the substrate atomic lattice.

## 5 $^3\text{He}$ in reduced dimensions

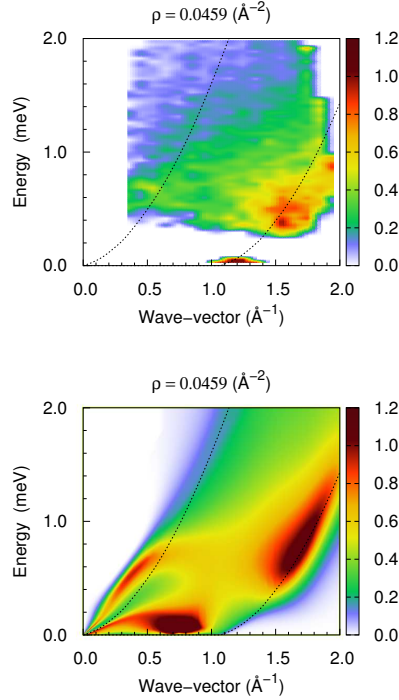


Figure 11: Experimental (top) and theoretical (left) determinations of the dynamic structure factor of two-dimensional liquid  $^3\text{He}$  [66]. The theoretical calculation shows the density and spin-density modes; the latter is not visible experimentally, it is masked by a strong elastic signal due to the substrate. A comparison with Fig. 7 shows that the roton-like excitation in the 2D system is found outside the particle-hole band (the region limited by the blue solid lines), thus avoiding Landau damping.

The excitations in  $^3\text{He}$  films are shown in Fig. 11. They are very similar to those discussed above for bulk liquid, with the remarkable exception [66] that the roton-

like excitations are at the edge of the particle-hole band and hence not strongly affected by Landau damping. These excitations can therefore propagate, suggesting interesting physical effects specific to 2D Fermi liquids.

## 6 Summary

The investigation of the dynamics of quantum fluids has been performed experimentally at very low temperatures using various techniques, mainly specific heat, compressibility, neutron and X-ray scattering and, for  $^3\text{He}$ , nuclear magnetic susceptibility. Theoretical calculations are based on semi-phenomenological approaches [67, 68, 69], dynamic many body theory (DMBT) [43, 30, 44] as well as different versions of Quantum Monte Carlo numerical calculations (PIMC, DMC) [27, 29, 60, 57] to cite only a few. These have brought a very detailed understanding of these systems. It is sometimes very difficult to perform experimental measurements on some particular systems (for instance in reduced dimensionality), or even impossible to create quite arbitrary systems ("mathematical models" of interaction or external potentials, etc.). In this case the combination of numerical and microscopic techniques is essential.

The results find a natural application to many different physical systems, like nuclear matter, neutron stars, particle physics and cosmology, where strongly interacting particles are investigated. Particles themselves, in fact, can be interpreted as quantized excitations of an underlying field. The helium liquids have been, in some sense, the Ariadne thread in these investigations: Their interactions are well established [70, 71] and, compared to nucleon interactions, quite simple. The density of these systems is very high and they are very "quantum", hence they do not permit the simple treatments that have become popular by the experimental success to generate and investigate cold quan-

tum gases. The experimental challenge is equally high and only the very best of the experimental equipment and the experimental techniques can stand up to the challenge. Nevertheless, these challenges have been met on both the theoretical and experimental side.

## References

- [1] Fetter, A. L. and Walecka, J. D., *Quantum Theory of Many-Particle Systems*, McGraw-Hill, New York, 1971.
- [2] Thouless, D. J., *The quantum mechanics of many-body systems*, Academic Press, New York, 2 edition, 1972.
- [3] Pines, D. and Nozieres, P., *The Theory of Quantum Liquids*, volume I, Benjamin, New York, 1966.
- [4] Wilks, J., *The Properties of Liquid and Solid Helium*, Clarendon, New York, Oxford, 1967.
- [5] de Boer, J. and Michels, A., *Physica* **6** (1938) 945.
- [6] Aziz, R. A., Slaman, M. J., Koide, A., Allnatt, A. R., and Meath, W. J., *Mol. Phys.* **77** (1992) 321337.
- [7] de Boer, J., *Physica* **14** (1948) 139.
- [8] Kapitza, P., *Nature* **141** (1938) 74.
- [9] Misener, J. F. A. . A. D., *Nature* **141** (1938) 75.
- [10] London, F., *Nature* **141** (1938) 643.
- [11] Landau, L., *J. Phys. U.S.S.R.* **5** (1941) 71.
- [12] Landau, L., *J. Phys. U.S.S.R.* **11** (1947) 91.
- [13] Bogoliubov, N. N., *J. Phys. U.S.S.R.* **11** (1947) 23.
- [14] Feynman, R. P., *Phys. Rev.* **94** (1954) 262.
- [15] Feynman, R. P. and Cohen, M., *Phys. Rev.* **102** (1956) 1189.
- [16] Palevsky, H., Otnes, K., Larsson, K. E., Pauli, R., and Stedman, R., *Phys. Rev.* **108** (1957) 1346.
- [17] Palevsky, H., Otnes, K., and Larsson, K. E., *Phys. Rev.* **112** (1958) 11.
- [18] Glyde, H. R., *Rep. Prog. Phys.* **81** (2018) 014501.
- [19] Lovesey, S. W., *Theory of Neutron Scattering from Condensed Matter*, Clarendon Press, Oxford, 1984.
- [20] Glyde, H. R., *Excitations in liquid and solid helium*, Oxford University Press, Oxford, 1994.
- [21] Beauvois, K. et al., *Phys. Rev. B* **97** (2018) 184520.
- [22] Godfrin, H. et al., *Phys. Rev. B* **103** (2021) 104516.
- [23] Cowley, R. A. and Woods, A. D. B., *Can. J. Phys.* **49** (1971) 177.
- [24] Glyde, H. R., Gibbs, M. R., Stirling, W. G., and Adams, M. A., *Europhysics Letters* **43** (1998) 422.
- [25] Jackson, H. W. and Feenberg, E., *Rev. Mod. Phys.* **34** (1962) 686.
- [26] Lee, D. K. and Lee, F. J., *Phys. Rev. B* **11** (1975) 4318.
- [27] Boronat, J. and Casulleras, J., *Europhys. Lett.* **38** (1997) 291.
- [28] Boronat, J. and Casulleras, J., *J. Low Temp. Phys.* **110** (1998) 443.
- [29] Ferré, G. and Boronat, J., *Phys. Rev. B* **93** (2016) 104510.
- [30] Campbell, C. E., Krotscheck, E., and Lichtenegger, T., *Phys. Rev. B* **91** (2015) 184510/1.
- [31] Jackson, H. W. and Feenberg, E., *Ann. Phys. (NY)* **15** (1961) 266.
- [32] Jackson, H. W., *Phys. Rev.* **185** (1969) 186.
- [33] Jackson, H. W., *Phys. Rev. A* **8** (1973) 1529.
- [34] Jackson, H. W., *Phys. Rev. A* **9** (1974) 964.

- [35] Manousakis, E. and Pandharipande, V. R., Phys. Rev. B **33** (1986) 150.
- [36] Pitaevskii, L. P., Zh. Eksp. Theor. Fiz. **36** (1959) 1168, [Sov. Phys. JETP **9**, 830 (1959)].
- [37] Campbell, C. E. and Krotscheck, E., Phys. Rev. B **80** (2009) 174501.
- [38] Vitali, E., Rossi, M., Reatto, L., and Galli, D. E., Phys. Rev. B **82** (2010) 174510/1.
- [39] Roggero, A., Pederiva, F., and Orlandini, G., Phys. Rev. B **88** (2013) 094302.
- [40] Nava, M., Galli, D. E., Moroni, S., and Vitali, E., Phys. Rev. B **87** (2013) 144506/1.
- [41] Dobbs, E. R., *Helium Three*, Oxford University Press, Oxford, 2001.
- [42] Krotscheck, E., Phys. Rev. A **26** (1982) 3536.
- [43] Böhm, H. M., Holler, R., Krotscheck, E., and Panholzer, M., Phys. Rev. B **82** (2010) 224505.
- [44] Krotscheck, E. and Lichtenegger, T., Dynamic many body theory IV: (Spin-)density fluctuations and exchange in normal-liquid  $^3\text{He}$ , 2022, in preparation.
- [45] Glyde, H. R. et al., Phys. Rev. B **61** (2000) 1421.
- [46] Pines, D., Physics Today **34** (Nov. 1981) 106.
- [47] Fåk, B., Guckelsberger, K., Körfer, M., Scherm, R., and Dianoux, A. J., Phys. Rev. B **41** (1990) 8732.
- [48] Albergamo, F., Verbeni, R., Huotari, S., Vankó, G., and Monaco, G., Phys. Rev. Lett. **99** (2007) 205301/1.
- [49] Schmets, A. J. M. and Montfrooij, W., Phys. Rev. Lett. **100** (2008) 239601/1.
- [50] Albergamo, F., Verbeni, R., Huotari, S., Vankó, G., and Monaco, G., Phys. Rev. Lett. **100** (2008) 239602/1.
- [51] Krotscheck, E. and Panholzer, M., J. Low Temp. Phys. **163** (2011) 1.
- [52] Yano, H., Yoshizaki, S., Inagaki, S., Fukushima, Y., and Wada, N., J. Low Temp. Phys. **110** (1998) 573–578.
- [53] Kato, H., Ishioh, K., Wada, N., Ito, T., and Watanabe, T., J. Low Temp. Phys. **68** (1987) 321.
- [54] Maestro, A. D., Nichols, N. S., Prisk, T. R., Warren, G., and Sokol, P. E., Experimental realization of one dimensional helium, 2022, arXiv:2203.11984.
- [55] Stan, G. and Cole, M. W., Surface Science **395** (1998) 280.
- [56] Stan, G., Crespi, V. H., Cole, M. W., and Boninsegni, M., J. Low Temp. Phys. **113** (1998) 447–452.
- [57] Bertaina, G., Motta, M., Rossi, M., Vitali, E., and Galli, D. E., Phys. Rev. Lett. **116** (2016) 135302.
- [58] Krotscheck, E. and Miller, M. D., Phys. Rev. B **60** (1999) 13038.
- [59] Gordillo, M. C., Boronat, J., and Casulleras, J., Phys. Rev. B **61** (2000) R878.
- [60] Arrigoni, F., Vitali, E., Galli, D. E., and Reatto, L., Fizika Nizkikh Temperatur **39** (2013) 1021.
- [61] Krotscheck, E. and Lichtenegger, T., J. Low Temp. Phys. **178** (2015) 61.
- [62] Nozières, P., J. Low Temp. Phys. **137** (2004) 45.
- [63] Nozières, P., J. Low Temp. Phys. **142** (2006) 83.
- [64] Lauter, H. J., Godfrin, H., Frank, V. L. P., and Leiderer, P., Phys. Rev. Lett. **68** (1992) 2484.
- [65] Clements, B. E., Krotscheck, E., and Tymczak, C. J., Phys. Rev. B **53** (1996) 12253.
- [66] Godfrin, H. et al., Nature **483** (2012) 576.
- [67] Aldrich, C. H. and Pines, D., J. Low Temp. Phys. **25** (1976) 677.

- [68] Aldrich III, C. H. and Pines, D., J. Low Temp. Phys. **31** (1978) 689.
- [69] Hsu, W. and Pines, D., J. Stat. Phys. **38** (1985) 273.
- [70] Aziz, R. A., Nain, V. P. S., Carley, J. C., Taylor, W. J., and McConville, G. T., J. Chem. Phys. **70** (1979) 4330.
- [71] Aziz, R. A., McCourt, F. R. W., and Wong, C. C. K., Molec. Phys. **61** (1987) 1487.